J. Biochem. 2018;164(5):369–379 doi:10.1093/jb/mvy061

JB THE JOURNAL OF BIOCHEMISTRY

Chaperonin facilitates protein folding by avoiding initial polypeptide collapse

Received February 25, 2018; accepted July 12, 2018; published online July 23, 2018

Fumihiro Motojima[1,2,*,†], Katsuya Fujii[1,*] and Masasuke Yoshida[3]

[1]Department of Molecular Biosciences, Kyoto Sangyo University Kamigamo-Motoyama, Kita-ku, Kyoto 603-8555, Japan, [2]Biotechnology Research Center and Department of Biotechnology, Toyama Prefectural University, 5180 Kurokawa, Imizu, Toyama 939-0398, Japan, and [3]Institute for Protein Dynamics, Kyoto Sangyo University, Kamigamo-Motoyama, Kita-ku, Kyoto 603-8555, Japan

*Present addresses: Fumihiro Motojima, Fuji Chemical Industries Co., Ltd, 1 Gohkakizawa, Kamiichi-machi, Nakaniikawa-gun, Toyama 930-0397, Japan; Katsuya Fujii, Daiichi Yakuhin Kogyo Co., Ltd, Kusashima 15-1, Toyama, Toyama 930-2201, Japan.

[†]Fumihiro Motojima, Department of API and Pharmaceutical Development, Fuji Chemical Industries Co., Ltd., 1 Gohkakizawa, Kamiichi-machi, Nakaniikawa-gun, Toyama 930-0397, Japan. Tel: +81-76-472-5535, Fax: +81-76-472-5342, email: fmotojim@gmail.com

Chaperonins assist folding of many cellular proteins, including essential proteins for cell viability. However, it remains unclear how chaperonin-assisted folding is different from spontaneous folding. Chaperonin GroEL/GroES facilitates folding of denatured protein encapsulated in its central cage but the denatured protein often escapes from the cage to the outside during reaction. Here, we show evidence that the in-cage-folding and the escape occur diverging from the same intermediate complex in which polypeptide is tethered loosely to the cage and partly protrudes out of the cage. Furthermore, denatured proteins in the chaperonin cage are kept in more extended conformation than those initially formed in spontaneous folding. We propose that the formation of tethered intermediate of polypeptide is necessary to prevent polypeptide collapse at the expense of polypeptide escape. The tethering of polypeptide would allow freely mobile portions of tethered polypeptide to fold segmentally.

Keywords: chaperonin; collapsed state; GroEL; molecular chaperone; protein folding.

Abbreviations: BFP, blue fluorescence protein; DMMBP, double-mutant (V8G/Y283D) of maltose-binding protein (MBP); DTT, dithiothreitol.

Many cellular proteins require the assistance of molecular chaperones when they fold into the native structure. The system of a bacterial chaperonin from *Escherichia Coli*, GroEL/GroES, a molecular chaperone that has been studied extensively, assists folding of nascent or denatured proteins in an ATP-dependent manner. GroEL consists of two rings stacked back-to-back. Each ring containing seven 57-kDa subunits forms a large central cavity. GroES is a dome-shaped heptameric ring of 10-kDa subunits. GroEL binds denatured protein at the hydrophobic apical end of the central cavity. Upon binding of ATP to GroEL, GroES attaches to the apical end of GroEL ring as a lid. Then denatured protein is encapsulated into the closed cavity (cage) and starts folding. After several seconds coupled with ATP hydrolysis, the lid GroES is detached and the encapsulated substrate protein, folded or not, becomes free in bulk solution (*1*, *2*).

Several models have been proposed to explain chaperonin-assisted folding. According to the passive Anfinsen cage model, proteins fold in spontaneous manner in the cage without a risk of aggregate formation (*3*, *4*). The iterative annealing model assumes that repetitive binding and release of denatured protein to and from GroEL induces annealing of a misfolded intermediate, thereby enabling its folding into its native state (*5*, *6*). The confinement model points out that the restriction of the conformational variety of denatured protein in the narrow cage accelerates protein folding by decreasing the activation entropy (*7*, *8*). Any of the models described above include the assumption that a whole polypeptide in the cage is enclosed entirely and it is completely isolated from environment. However, our previous studies show that the denatured protein in the cage is accessible from outside by protease, antibody against the protein, and trap(N265A), a GroEL mutant with a strong binding affinity to denatured protein (*9*, *10*). Often, it even escapes out of the cage. Actually, polypeptide in the cage is loosely and non-covalently tethered to the hydrophobic interfaces of GroES/GroEL and GroEL subunits, and partially threading out of the cage through the interfaces (*10*). Several residues of GroEL located at the interfaces between GroEL/GroES and between GroEL subunits are identified to be involved in the tethering and their mutation affect protein folding (*10*). Although there appears little space at the interfaces in the crystal structure (*11*), gaps at the interfaces are formed by structural fluctuation as observed by electron microscopy (*12*). Also the hydrophobic C-terminal peptides of GroEL may contribute the tethering as suggested (*12*, *13*). The finding that denatured protein is always tethered on the chaperonin cage is a contrast to the previous models in which denatured protein is compacted in the cage (confinement model) and it is extended transiently upon GroES binding (iterative annealing model). It is assumed that tethering enables protein folding from extended conformation, not from collapsed conformation formed in spontaneous folding.

© The Author(s) 2018. Published by Oxford University Press on behalf of the Japanese Biochemical Society.
This is an Open Access article distributed under the terms of the Creative Commons Attribution Non-Commercial License (http://creativecommons.org/licenses/by-nc/4.0/), which permits non-commercial re-use, distribution, and reproduction in any medium, provided the original work is properly cited. For commercial re-use, please contact journals.permissions@oup.com

However, the effect of tethering on the folding assistance mechanism of chaperonin has not been experimentally elucidated yet.

In addition to tethering, we previously found that a denatured protein in the cage follows two pathways: it folds in the cage (in-cage folding) or it escapes out of the cage, followed by spontaneous folding (out-of-cage folding) (*10*, *14*, *15*). However, it has been unknown whether two pathways are diverged from a unique tethered intermediate or their independent intermediates. If a unique intermediate exists, tethered intermediate can be analysed from observations at the beginning of chaperonin-assisted folding. Herein, we present kinetic evidence for the presence of an initial common tethered intermediate from which the two pathways diverge. Real-time observation of the folding of blue fluorescence protein (BFP) revealed that BFP folds through two successive reactions including near-native intermediate, whereas it folds through single reaction in spontaneous folding. We found that tethering physically extends denatured protein in the cage and prevents denatured proteins from the initial compaction that usually occurs in spontaneous folding. The salient implication is that chaperonin can assist efficient folding by formation of the tethered intermediate, which physically prevents the hydrophobic collapse of the whole polypeptide and allows free segments to undergo productive folding.

Materials and Methods

Proteins

The mutants of proteins used in this study were prepared using QuikChange multi Lightning Site-Directed Mutagenesis Kit (Agilent Technologies Inc.) with appropriate oligonucleotides. The mutants of GroEL, GroES, and fluorescently labelled GroES were prepared as described (*10*, *14*, *16*). Concentrations of GroEL, SR1, SR398 and GroES are those of their oligomeric form in this article. Cysteine-less BFP was prepared by the mutations of C49A, F65L, Y67H and C71V in wild-type green fluorescence protein (GFP). MBP, double-mutant (V8G/Y283D) of maltose-binding protein (DMMBP) and DapA from *E. coli* were prepared as described (*10*, *14*, *17*). The concentration of DapA is shown as monomer.

BFP folding assays

The reaction mixture containing 0.1 μM GroEL or SR398 and 0.5 μM GroES in buffer HKM (50 mM HEPES-NaOH, pH 7.5, 50 mM KCl, 10 mM $MgCl_2$, and 1 mM DTT) was incubated with stirring in a quartz cuvette placed in a water jacket with circulating water at the indicated temperature. BFP was denatured by adding an equal volume of 200 mM glycine-HCl pH 2.5. Denatured BFP (10 μM) was added to the reaction mixture at the final concentration of 0.05 μM. For fluorescently labelled BFP, the final concentration was 0.02 μM. ATP was added to start chaperonin-assisted folding. To measure BFP folding in the chaperonin cage, 0.1 μM trap(D87K) was mixed before ATP addition to eliminate free denatured BFP that had escaped from the cage to the bulk solution. BFP folding was monitored by the fluorescence emission of 440 nm excited at 380 nm using a fluorometer (FP-6500; Jasco Corp.). In rapid-mixing experiment (SFM-400; Biologic), 1.0 μM GroES was used.

Rubisco folding assay

Rubisco was denatured in urea as reported (*14*). Denatured Rubisco (final 1 μM) was diluted by 50-fold into buffer H5KM (50 mM HEPES-NaOH, pH 7.5, 5 mM KCl 10 mM $MgCl_2$, and 1 mM DTT) containing 2 μM SRKKK2, 4 μM GroES, 10 mM glucose, and 10 mM $NaHCO_2$. The folding reaction was started by addition of ATP (final = 1 mM). At 10 s after ATP addition, excess ATP was hydrolyzed to ADP by addition of hexokinase (final = 0.01 U/μl). For the experiment of refolding of heat-denatured Rubisco within the cage, the SRKKK2 containing native Rubisco monomer in the cage produced as described above was incubated at 45°C for 15 min. For rapid temperature shift from 45 to 25°C, the reaction solution was mixed into a micro tube containing the equal volume of buffer H5KM preincubated at 25°C. Generation of native Rubisco monomer was assayed as follows. Aliquots (20 μl) were mixed with ice-cold quenching buffer (40 μl) containing 20 mM Tris-HCl pH7.5, 15 mM EDTA, 1 mM DTT and 0.5 μM trap(D87K). BSA was subsequently added to aliquots (final 0.2 mg/ml) and frozen by liquid nitrogen. The thawed samples on ice were activated and their Rubisco activity were measured by coupled enzyme assay as reported (*14*).

Gel filtration analysis of BFP

The folding reaction mixture was applied to Superdex 200 10/300 equilibrated with buffer containing 20 mM Tris-HCl pH 7.5, 5 mM KCl, 10 mM $MgCl_2$, and 1 mM DTT. Fluorescence of BFP was monitored using an in-line fluorometer (FP-2020; Jasco Corp.).

Fluorescence resonance energy transfer (FRET) observation to monitor the escape

The FRET efficiency change of a donor-labelled substrate protein upon binding to trap(D87K) labelled with TexasRed-maleimide ($trap(D87K)_{Tx}$) was measured as reported (*10*). BFP and DMMBP were denatured as described (*10*). DapA was denatured in solution containing 8 M urea, 2 mM DTT and 100 mM Tris-HCl pH7.5. Denatured substrate protein (final = 0.02 μM) was added to the buffer HKM containing 0.05 μM GroEL or 0.1 μM SR-variant at 25°C. When DapA was a substrate protein, 10 mM pyruvate was added and incubated at 20°C. Then, 0.5 μM GroES, 1 mM ATP and 0.1 μM $trap(D87K)_{Tx}$ for donor fluorescence change in the presence of acceptor TexasRed dye (F_{DA}) or non-labelled trap(D87K) for donor fluorescence change in the absence of acceptor (F_D) were added to start the assisted folding reaction. The percentage of FRET change was calculated from division of FRET efficiency ($1-F_{DA}/F_D$) by maximum FRET efficiency that was obtained when donor-labelled substrate proteins directly bound to $trap(D87K)_{Tx}$. In the case of BFP and DMMBP, the FRET efficiency change of SR398(E315C) labelled with Alexa Fluor 488 C_5-maleimide as donor fluorescence dye ($SR398(E315C)_{Alexa}$, 0.05 μM) and acceptor-labelled substrate protein (0.1 μM) upon escape out of the cage of $SR398(E315C)_{Alexa}$ was also measured. In rapid-mixing experiments, 1.0 μM GroES was used.

Fluorescence labelling for single-pair FRET

For single-pair FRET, we prepared mutants containing only two reactive cysteine residues that were located near each other in the native structure. Labelled proteins, donor dyes and acceptor dyes were the following: BFP(K52C/E172C) and BFP(K3C/239C), Alexa Fluor 488 C_5-maleimide (ThermoFisher Scientific) and tetramethylrhodamine-maleimide (ThermoFisher Scientific); DMMBP(D184C/K362C) and DapA(C20A/T3C/E223C), Alexa Fluor 350 C_5-maleimide (ThermoFisher Scientific) and ATTO488-maleimide (ATTO Tec.). First, donor fluorescence dye containing maleimide moiety was mixed into protein at 1:2 molar ratio and incubated for 1 h at 25°C. The donor-labelled protein was purified using gel filtration (Sephadex G-25, GE healthcare) to remove free fluorescence dye. Half of the purified product was reserved as donor-labelled sample. The other half of the donor-labelled protein was mixed with 4-fold molar excess of the acceptor fluorescence dye containing maleimide moiety. After incubation for 16 h at 4°C, free fluorescence dye was removed using gel filtration to purify donor–acceptor-labelled protein.

Measurement of single-pair FRET

Single-pair FRET was measured at 25°C (BFP and DMMBP) or at 20°C (DapA). The concentration of BFP, DMMBP and DapA were 0.05, 0.005 and 0.05 μM unless otherwise noted. In the case of DapA, buffer HKM was added with 10 mM pyruvate and 50 mM KCl (final 100 mM). Denatured proteins were diluted into the buffer and refolded as described above. In case of DapA, to inhibit FRET among DapA subunits in native tetramer, the labelled DapA was mixed with the 4-fold molar of non-labelled DapA and denatured. FRET efficiency (E_{FRET}) was calculated from the two fluorescence measurements using donor-labelled protein (F_D) and donor–acceptor-labelled protein (F_{AD}) using the function ($E_{FRET} = 1 - (F_{DA}/F_D)$).

Results

In-cage and out-of-cage folding diverge from the common tethered intermediate

We have demonstrated that denatured protein in the chaperonin cage folds in the cage (in-cage folding) or escapes out of the cage followed by spontaneous folding in the bulk solution (out-of-cage folding) (*10*, *14*). The reaction scheme by which in-cage and out-of-cage folding pathways diverge from the common tethered intermediate has been proposed (Tethering model, Fig. 1) (*10*, *15*). However, other possibilities remain such that each pathway has its own precursor intermediate formed upon GroES binding (Independent intermediate model, Supplementary Fig. S1). The differences of these models appear in their rate equations of in-cage folding and out-of-cage folding as described below. The first reaction, GroES binding, is not included in the equations, since it is much more rapid than other reactions in the scheme ($k = 3.0 \times 10^7$ M^{-1} s^{-1}, $t_{1/2}$ ~0.043 s at 0.5 μM GroES) (*16*). The in-cage folding is assumed to be a two-step reaction (**D**→**I**→**F**) as observed in out-of-cage folding (**D**→**E**→**N**) (Fig. 1). **I** and **E** are generated from the common intermediate **D** and their productions are typical competitive reactions. Therefore, total concentration of the produced states in the in-cage folding ([**I**] + [**F**]) and that of out-of-cage folding ([**E**] + [**N**]) by the time t are described as Equations (1) and (2) with the rate constant relationship shown by Equation (3).

$$[\mathbf{I}] + [\mathbf{F}] = (k_{in}/k_{app})[\mathbf{D}]_0\{1 - \exp(-k_{app}t)\} \quad (1)$$

$$[\mathbf{E}] + [\mathbf{N}] = (k_{out}/k_{app})[\mathbf{D}]_0\{1 - \exp(-k_{app}t)\} \quad (2)$$

$$k_{app} = k_{in} + k_{out} \quad (3)$$

$[\mathbf{D}]_0$ stands for the initial concentration of denatured protein bound on GroEL or its single-ring variant. As seen, the apparent rate constant of the in-cage release and that of the escape are the same (k_{app}). k_{in} and k_{out} signify an authentic rate constant of the in-cage release and that of the escape, respectively. It is noteworthy that the apparent rate constant k_{app} becomes the sum of the authentic rate constants of k_{in} and k_{out}. The authentic rate constants are obtained from the apparent rate constant k_{app} ($= k_{in} + k_{out}$) and the fraction of the final yield of the in-cage and out-of-cage folding (k_{in}/k_{app} and k_{out}/k_{app}, respectively). The production of **F** in the in-cage folding and that of **N** in the out-of-cage folding are described as two successive reactions shown in Supplementary Equations (S1) and (S2). The rate constant of the transition from **E** to **N** should be equal to that of spontaneous folding (Fig. 1). If in-cage folding and out-of-cage folding are independent, their apparent rates and yields have no relationship (Supplementary Fig. S1). Therefore, we analysed the kinetics of in-cage folding and the escape of denatured protein to discern the tethering model.

To test whether these relationships of the rates are really observed, we analysed the in-cage folding and

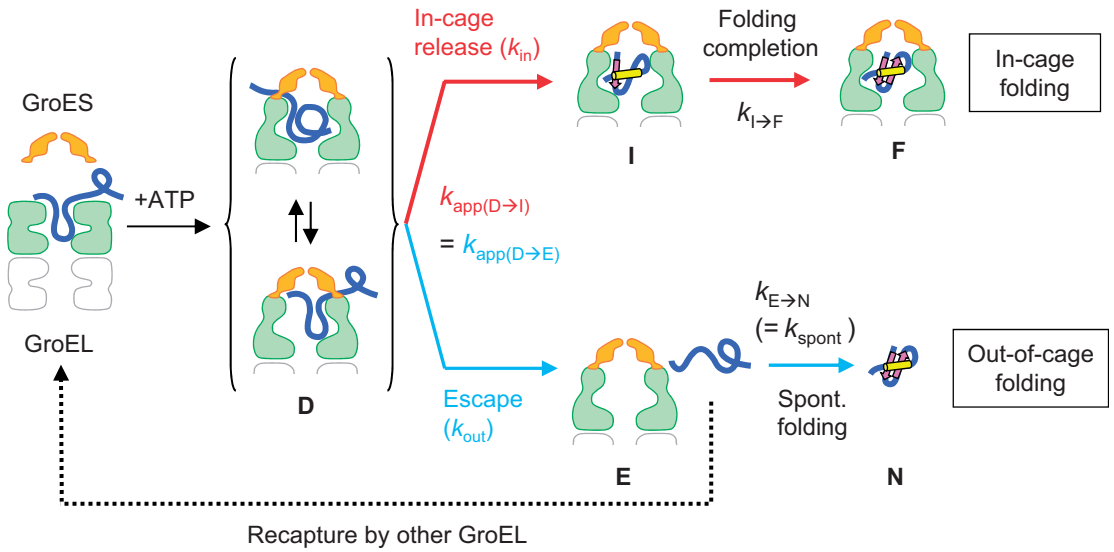

Fig. 1 The tethered intermediate scheme of chaperonin-assisted protein folding. Tethered intermediate scheme of chaperonin-assisted protein folding and its kinetic predictions. Dissociation of GroES from GroEL accompanied by ATP hydrolysis is not shown in this scheme. The recapture of escaped denatured protein by other GroEL is shown in dotted line. Tethered intermediate (**D**) is an ensemble of the heterogeneous species in dynamic equilibrium, in which tethering interaction site(s) in the polypeptide chain and in the cage wall are shifting quickly. In-cage folding and out-of-cage folding compete for **D**. In-cage folding includes in-cage release, in which the tethered polypeptide is released into the cage to generate an intermediate (**I**), and completion of folding, in which the polypeptide in the cage gains native structure (**F**). Out-of-cage folding includes escape of the tethered polypeptide out of the cage as a denatured protein (**E**) and spontaneous folding to native structure in the medium (**N**). In the case of wild-type GroEL, denatured protein is released to outside from chaperonin cage by escape or by ATP hydrolysis-coupled dissociation of GroES. In either case, most of denatured protein in the medium is recaptured by other GroEL since the binding of denatured protein and GroEL is very fast ($k = 1$–2×10^7 $M^{-1}s^{-1}$) (*21*). If this scheme is really the case, in-cage-release and escape occur apparently at the same rate ($k_{app(D→I)} = k_{app(D→E)}$), and $k_{E→N}$ is equal to the rate of spontaneous folding (k_{spont}). k_{in} is the authentic rate constant for the in-cage release and k_{out} is that of the escape.

out-of-cage folding of BFP. We used a cysteine-less variant of BFP(C49A/C71V), which is designated as BFP hereinafter if not otherwise noted. The spontaneous folding of BFP obeyed single exponential kinetics (k_{spont} = 1.14 min^{-1}), whereas GFP folds in two-phasic manner (*7*, *18*). To observe the single-turnover folding reaction, we used a single-ring version of GroEL, SR398, which includes a mutation of D398A that makes ATP hydrolysis very slow (*19*). Once GroES binds to the SR398-denatured protein binary complex upon ATP addition, it remains bound throughout whole period of the folding reaction (*10*, *14*, *19*). We previously reported that out-of-cage folding is inhibited by the low concentration of trap(D87K) (0.1 μM) without affecting in-cage folding (*10*, *14*). Regarding gel filtration analysis of the reaction mixture of SR398-assisted folding after folding reactions finished, two BFP fluorescent peaks, the SR398-GroES-BFP ternary complex (45% of total BFP) and free BFP (55%), appeared (Fig. 2A), as observed previously for GFP folding (*10*, *20*). The free BFP peak disappeared in the experiment in which trap(D87K) was added immediately before addition of ATP to start folding reaction, indicating that, in the absence of trap(D87K), BFP in a denatured state escapes from the cage and folds spontaneously to produce native BFP in the bulk solution.

The time course of the escape of denatured BFP into the bulk solution was monitored by the increase in FRET efficiency induced by the binding of donor-labelled BFP ($BFP(E172C)_{Alexa}$) to acceptor-labelled trap(D87K) ($trap(D87K)_{Tx}$) in the bulk solution (Fig. 2B, cyan). After the start of the reaction, FRET efficiency increased with a single exponential function, giving the apparent rate ($k_{app(D\rightarrow E)}$ = 2.63 min^{-1}) and levelled off at the escaped fraction (47%). The escape of denatured BFP from the cage was also monitored using FRET between donor-labelled SR398 ($SR398(E315C)_{Alexa}$) and acceptor-labelled BFP ($BFP(E172C)_{TMR}$) in the absence of trap(D87K) (Fig. 2B, blue). Again, the apparent rate $k_{app(D\rightarrow E)}$ = 2.52 min^{-1} was obtained. The initial rapid decrease of FRET upon ATP addition would reflect the

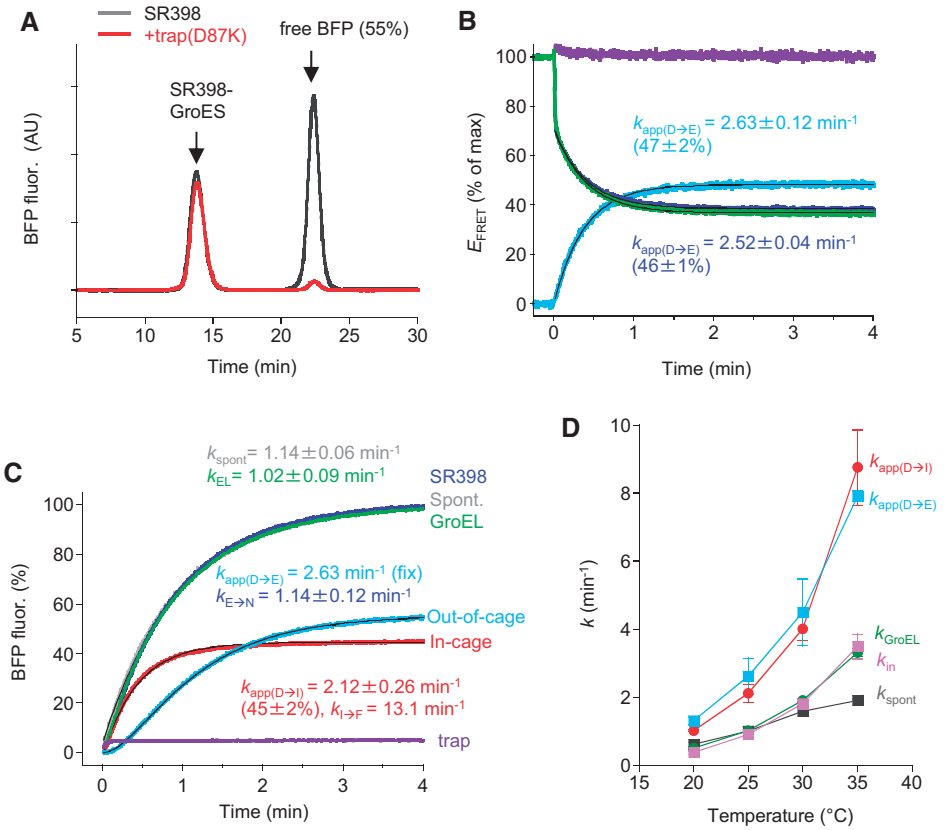

Fig. 2 Chaperonin-assisted folding of BFP. **(A)** Gel filtration analysis of SR398-assisted BFP folding in the absence (SR398, grey) or presence of trap(D87K) (+trap(D87K), red). **(B)** Time course of the escape of BFP measured by FRET. ATP (final 1 mM) was added to start the reaction at time 0. Cyan, FRET between donor-labelled $BFP(E172C)_{Alexa}$ and acceptor-labelled $trap(D87K)_{Tx}$ shown as percent of maximum FRET efficiency obtained when denatured BFP was added to $trap(D87K)_{Tx}$/GroES/ATP (purple). Blue and green, FRET between donor-labelled $SR398(E315C)_{Alexa}$ and acceptor-labelled $BFP(E172C)_{TMR}$ in the absence and presence of trap(D87K), respectively, shown as percent of maximum FRET efficiency before ATP addition. The fitting curves giving the indicated rate constants are coloured in black. The escape yield is estimated from the ratio between E_{FRET} value at 4 min and that immediately after ATP addition. **(C)** BFP folding assisted by SR398 at 25°C. ATP (final 1 mM) was added to start the reaction at time 0. Blue, SR398-assisted folding; green, GroEL-assisted folding; grey, spontaneous folding; red, in-cage folding (folding in the presence of trap(D87K)); cyan, out-of-cage folding ([blue curve]-[red curve]); purple, spontaneous folding in the presence of trap(D87K)/GroES/ATP. The fitting curves giving the indicated rate constants are coloured in black. **(D)** The observed rate constants of BFP folding at various temperatures. $k_{app(D\rightarrow I)}$ was obtained from the in-cage folding of BFP. $k_{app(D\rightarrow E)}$ were obtained from the out-of-cage folding of BFP when $k_{E\rightarrow N}$ is fixed to k_{spont}; k_{GroEL} is a rate constant of GroEL-assisted folding simulated as a single exponential function; k_{in} was calculated from the Equation (1). The rate constants averaged from three independent experiments and their standard deviations are shown.

distance increase upon the conformational change of SR398 induced by GroES-ATP binding. No initial lag phase exists in the reactions (Supplementary Fig. S2A), confirming that **D** is an immediate product of encapsulation and that it is a direct precursor of the escape. The escaped fraction was calculated by the decreased FRET value (32%) at 4 min from the initial FRET value upon ATP binding (70%) and gave 46% that was consistent with the value obtained from FRET between BFP and trap(D87K) (Fig. 2B, cyan). Thus, it is considered that disappearance of denatured BFP from the cage and appearance of denatured BFP in the bulk solution take place at the same apparent rate constant, which corresponds to k_{app} in Equation (2). In these experiments, inclusion of non-labelled trap(D87K) in the mixture did not change the kinetics (Fig. 2B, green), thereby confirming that trap(D87K) did not affect the escape kinetics. Free denatured BFP rapidly bound to trap(D87K) in <2 s (Fig. 2B, purple) and its folding was inhibited (Fig. 2C, purple). The binding of denatured protein to trap(D87K) is expected to be as rapid as that to GroEL ($k = 1–2 \times 10^7$ $M^{-1}s^{-1}$, apparent rate at 0.1 μM GroEL is ~1 s^{-1}) and this is much faster than protein escape ($k_{app(D\rightarrow E)} = 2.52$ min^{-1}) (*21*). Thus, FRET change reflects the escape of denatured protein in these experiments. Fluorescence labelling used in these experiments did not cause a marked change of folding kinetics of BFP at 25°C (Supplementary Fig. S2B).

Direct monitoring of in-cage and out-of-cage folding

BFP folding assisted by SR398 can be monitored directly by the fluorescence recovery of BFP at time resolution ~0.1 s, enabling us to determine all the rates of in-cage and out-of-cage folding for the first time. Folding in the presence of trap(D87K) (Fig. 2C, red), which represents in-cage folding, has a short lag (Supplementary Fig. S2C) and is fitted well by two successive reactions with apparent rate constants: 2.12 min^{-1} and 13.1 min^{-1} (Supplementary Equation S1). The former value is close to the rate of the escape obtained from FRET (2.52 min^{-1}). Therefore, it is assumed to be the rate of in-cage release $k_{app(D\rightarrow I)}$. Then, the latter would be the rate of generation of native BFP in the cage ($k_{I\rightarrow F}$). This reaction sequence is opposite from that proposed previously (*22*, *23*). The value of $k_{I\rightarrow F}$ is one order larger than that of k_{spont}. BFP released into the cage is likely to have a near-native structure already so that it can gain a native structure very rapidly. In contrast, there is no lag phase in spontaneous folding of BFP (Supplementary Fig. S2C). This implies that the folding pathway of BFP in the chaperonin cage is changed from that in spontaneous folding even though the authentic in-cage folding rate of k_{in} is similar to k_{spont} at 25°C.

The time course of the out-of-cage folding (Fig. 2C, cyan), which was obtained by subtraction of the in-cage folding from the folding in the absence of trap(D87K) ([blue curve]–[red curve]), has a long lag phase, implying two successive reactions with the apparent rate of denatured BFP escape ($k_{app(D\rightarrow E)}$) and the folding rate of escaped BFP ($k_{E\rightarrow N}$) (Fig. 1). When the apparent rate constant of $k_{app(D\rightarrow E)}$ (2.63 min^{-1}) obtained from the escape measurement by FRET (Fig. 2B) is applied as a fixed parameter to the formula of two successive reactions (Supplementary Equation S2), the rate constant $k_{E\rightarrow N} = 1.14$ min^{-1} gives the best simulation. This value is equal to the rate of spontaneous folding ($k_{spont} = 1.14$ min^{-1}). These results all satisfy Equations (1) and (2) and justify the scheme presented in Fig. 1.

BFP folding at various temperatures

The experiments above mentioned were carried out at 25°C. If the tethering scheme for the chaperonin mechanism is true, relations $k_{app(D\rightarrow I)} = k_{app(D\rightarrow E)}$ and $k_{E\rightarrow N} = k_{spont}$ should be observed under any conditions. To examine this, we repeated the same experiments as Fig. 2B and C but at different temperatures, 20, 30 and 35°C (Supplementary Fig. S2D and E) and the rates were compared (Fig. 2D). The value of $k_{app(D\rightarrow I)}$ was calculated from the in-cage folding of BFP in the presence of trap(D87K). The value of $k_{app(D\rightarrow E)}$ was calculated from the out-of-cage folding of BFP according to Supplementary Equation (S2) by using the value of $k_{E\rightarrow N}$ as k_{spont}. The values of $k_{app(D\rightarrow I)}$ and $k_{app(D\rightarrow E)}$ are very similar and we consider that they are close enough to meet Equations (1) and (2). The rate constants of BFP folding assisted by wild-type GroEL (k_{GroEL}) were very close to k_{in}, but not to $k_{app(D\rightarrow I)}$ of SR398-assisted folding (Fig. 2D), and this reason is also explained by the tethering scheme. In the case of GroEL, out-of-cage folding actually does not occur because an escaped BFP in denatured state is recaptured before it folds spontaneously by other GroEL molecule to enter the next cycle of chaperonin reaction (Fig. 1). Without a competing out-of-cage folding reaction, GroEL-assisted folding proceeds only by a manner of in-cage folding at the rates of k_{in} and $k_{I\rightarrow F}$. Because the second step of the in-cage folding is very rapid as described, the overall rate of GroEL-assisted folding (k_{GroEL}) is mostly determined by the first step and is expected to be nearly equal to k_{in}. This agreement also indicates that the iterative ATPase cycle of GroEL does not accelerate BFP folding. It is interesting that the rate of spontaneous folding is not elevated significantly above 30°C and chaperonin-assisted BFP folding, approximated by k_{in}, is two times more rapid than spontaneous folding at 35°C. The slow spontaneous folding at 35°C is not attributable to the formation of reversible aggregate because the rate and yield of spontaneous BFP folding at 35°C are unaffected by BFP concentrations (Supplementary Fig. S2F).

Refolding of protein denatured within the cage

Even if chaperonin-assisted folding proceeds through the tethered intermediate (**D** in Fig. 1), a question remains whether **D** is formed only through ATP-induced GroES binding. To test this, we observed whether the tethered intermediate **D** is formed when a denatured protein is generated within the cage, but not through GroES binding. As Apetri *et al.* (*24*) reported for dehydrofolate reductase, in-cage denaturation is achieved by exposing a native protein in the cage to a high, but chaperonin-durable, temperature and refolding is initiated by temperature shift-down. We used a

single-ring GroEL mutant, SRKKK2, which does not release GroES at 45°C (Supplementary Fig. S3), and Rubisco as an obligate substrate protein of chaperonin which is denatured at 45°C without escaping from the cage. A native Rubisco monomer folded in the SRKKK2's cage was heat-denatured completely at 45°C and then refolding was monitored at 25°C. It was established that Rubisco is folded in the cage without escaping the cage at 25°C (*10*). Refolding kinetics of heat-denatured Rubisco in the cage is very similar to that of the control urea-denatured Rubisco encapsulated in the cage by GroES binding with final yields around 100% and rates around 0.12 min^{-1} (Fig. 3). Either for heat-denatured or urea-denatured Rubisco, refolding was inhibited in a short time when trap(N265A) was added to the reaction medium at 1 min after the start of refolding reaction. Trap(N265A) has strong affinity to unfolded polypeptide and, different from trap(D87K), it can bind to a portion of Rubisco polypeptide protruding out of the cage under the conditions, thereby preventing further refolding (*9*, *10*). These results show that the tethering is an inherent reaction of chaperonin that occurs simply when denatured protein is present in the cage, but not dependent on the process of encapsulation.

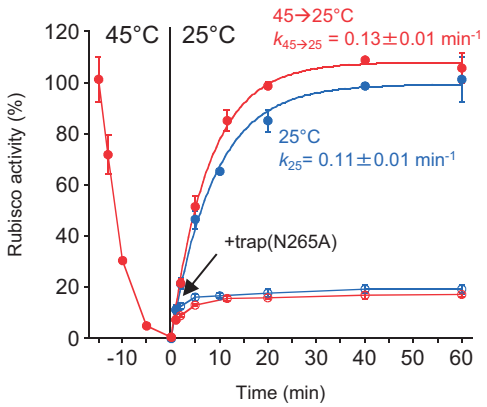

Fig. 3 Refolding of Rubisco denatured within the cage. Blue circles: Folding of urea-denatured Rubisco monomer was started by ATP-induced GroES binding to SRKKK2 at 25°C. Red circles: A native Rubisco monomer in the cage of SRKKK2 was heat-denatured by incubation at 45°C (−15 to 0 min), and refolding in the cage was started by a temperature shift to 25°C. Open circles: The folding of Rubisco after addition of trap(N265A) (2 μM) at 1 min. Standard deviations from three independent experiments are shown. Other experimental details are described in Material and Methods section.

Tethering prevents polypeptide collapse in BFP folding

The conformational state of BFP during folding was probed using single-pair FRET. Cysteine residues of BFP(K52C/E172C) (Fig. 4A) were labelled by donor (Alexa488) and acceptor (tetramethylrhodamine) fluorescent dyes and the change of FRET efficiency was monitored. Depending on the distance of the two dyes, FRET efficiency became minimum when BFP was denatured in acid (E_{FRET} = 0.32 ± 0.01) and it became maximum when BFP was in a native state in bulk solution (E_{FRET} = 0.95 ± 0.01) and in the cage (E_{FRET} = 0.95 ± 0.01) (Supplementary Fig. S4A). In spontaneous folding, the initial FRET efficiency was 0.86 ± 0.01, which increased slowly to 0.95 of the native state at the rate 0.90 min^{-1} (Fig. 4B). The curves of FRET efficiency change in two different concentrations of BFP were the same (Fig. 4B, cyan and blue), indicating that high initial E_{FRET} is not caused by aggregation formation. This high initial E_{FRET} value suggests that, as observed in spontaneous folding of many proteins (*25–28*), the freely extending polypeptide of denatured BFP collapses to compact conformations immediately upon initiation of folding reaction. In contrast, and in support of the tethering scheme, the initial FRET efficiency of the SR398-assisted folding reaction (E_{FRET} = 0.77 ± 0.01) was lower than that of spontaneous folding, indicating that tethered polypeptide is extended. The rate of FRET efficiency change was 1.38 min^{-1}. As the tethered BFP is released into or outside of the cage and folds to the native structure, the FRET efficiency increases to the level of native BFP. The fact that no lag phase was observed in single-pair FRET indicates that

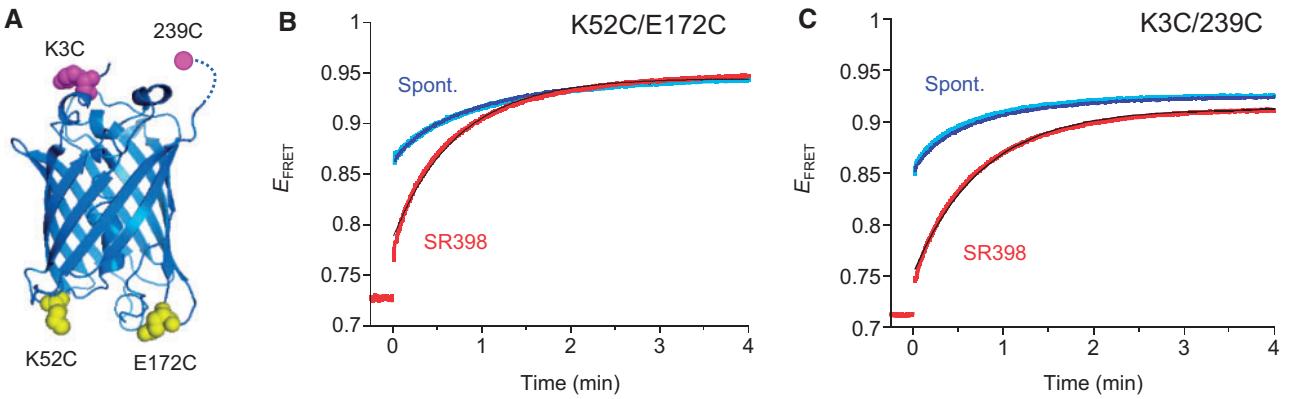

Fig. 4 Conformational change of BFP in chaperonin-assisted folding. **(A)** The residues mutated to cysteine for single-pair FRET. Crystal structure (PDB ID: 1GFL) of GFP is shown in cartoon model. The mutated residues of K52C/E172C and K3C/239C are shown in yellow and magenta CPK models, respectively. BFP folding monitored by the change of single-pair FRET efficiency (E_{FRET}) between fluorescent dyes labelled at K52C/E172C **(B)** and K3C/239C **(C)**. Spontaneous folding of 0.025 and 0.05 μM BFP are shown in cyan and blue curves, respectively. SR398-assisted folding is shown in red curves. Reactions were started at time zero by dilution of denatured BFP in spontaneous folding or by ATP-addition in SR398-assisted folding.

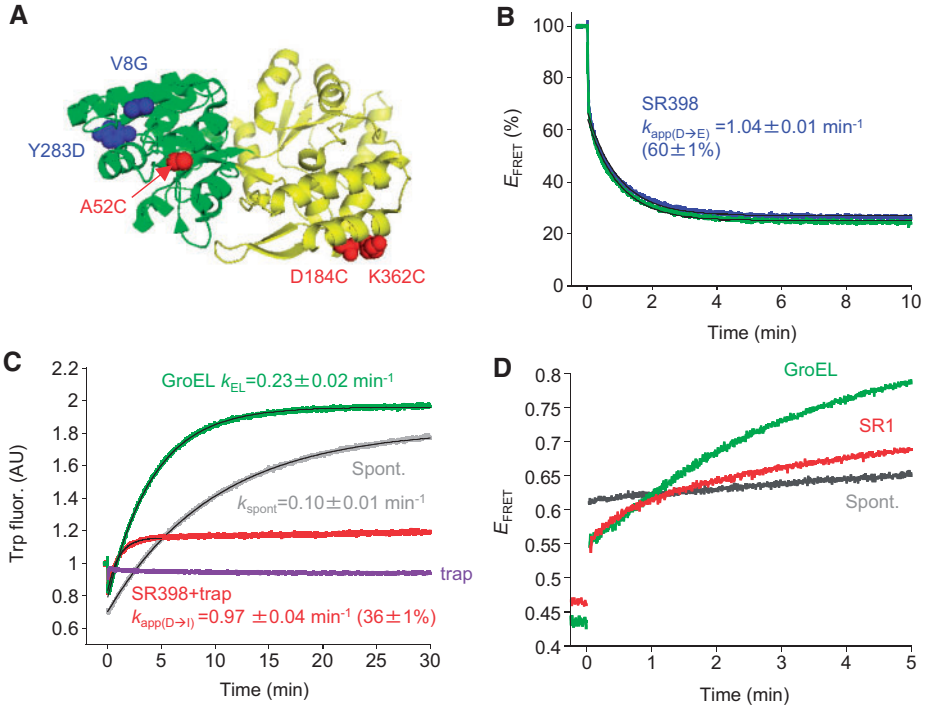

Fig. 5 Chaperonin-assisted folding of DMMBP. **(A)** Mutated residues of DMMBP used for this study. The crystal structure of MBP (PDB ID: 1OMP) is shown in cartoon model. The double-mutation (V8G/Y283D) and cysteine mutation (A52C, D184C and K362C) are coloured in blue and red, respectively. **(B)** Time course of the escape of DMMBP. FRET between donor-labelled SR398(E315C)$_{Alexa}$ and acceptor-labelled DMMBP(A52C)$_{Cy3}$ in the absence (blue) or presence of trap(D87K) (green) are shown as percent of maximum FRET efficiency before ATP addition. ATP (final 1 mM) was added to start the reaction at time 0. The fitting curves giving the indicated rate constants are coloured in black. The yield of in-cage folding shown in parentheses was estimated from E_{FRET} as described in Results (60%). **(C)** DMMBP folding monitored by recovery of tryptophan fluorescence of native DMMBP. Folding of urea-denatured DMMBP(A52C)$_{Cy3}$ was observed. Spontaneous folding, GroEL-assisted folding, in-cage folding assisted by SR1 in the presence of trap(D87K), spontaneous folding in the presence of trap(D87K)/GroES/ATP are shown in grey, green, red and purple, respectively. The in-cage folding yield is estimated based on the observation that magnitude of tryptophan fluorescence of native DMMBP in the chaperonin cage is 78% of that of free native DMMBP (*14*). **(D)** DMMBP folding monitored by the change of single-pair FRET efficiency (E_{FRET}) between fluorescent dyes labelled at D184C/K362C. Spontaneous folding, SR1-assisted folding, and GroEL-assisted folding are shown in grey, red and green, respectively. Reactions were started at time zero by dilution of denatured DMMBP in spontaneous folding or by ATP-addition in SR398-assisted folding.

I has a near-native conformation and the FRET efficiency of **I** is as high as that of **F**. Similar results were obtained from another FRET pair K3C/239C (Fig. 4C).

Folding of DMMBP obeys the tethering scheme

We examined next the folding of a DMMBP (Fig. 5A). DMMBP has been known as a typical protein of which folding is accelerated by chaperonin several times compared with spontaneous folding (*8*, *14*, *29*). Time course of the escape of DMMBP from the chaperonin cage was monitored by the decrease of FRET efficiency between SR398(E315C)$_{Alexa}$ and DMMBP(A52C)$_{Cy3}$. As the case of BFP, the initial rapid decrease of FRET upon ATP addition was observed. The subsequent slow decrease of FRET is defined by the apparent escape rate of $k_{app(D\rightarrow E)}$ (1.04 min^{-1}) (Fig. 5B). The escaped fraction was calculated by the decreased FRET value (40%) at 10 min from the initial FRET value upon ATP binding (67%) and gave 60% escape of DMMBP(A52C)$_{Cy3}$ out of the cage (Fig. 5B). Inclusion of trap(D87K) in the solution did not change the escape kinetics. In-cage folding of DMMBP(A52C)$_{Cy3}$ was monitored by the recovery of tryptophan fluorescence of native DMMBP in the presence of trap(D87K) (Fig. 5C). The spontaneous folding of free denatured DMMBP was completely inhibited in the presence of trap(D87K) (Fig. 5C, purple). Consistent with the escape fraction, the in-cage-folding yield was 36% (see Supplementary Material). The curve of fluorescence increase was well simulated by a single exponential function and an apparent rate 0.97 min^{-1} was estimated. The reason of no initial lag phase would be because the tryptophan fluorescence of DMMBP is insensitive to the structural change from **I** to **F**. Supporting this, the initial lag phase of MBP (~2 s) was observed by hydrogen exchanging mass analysis (*30*). Thus, the value of 0.97 min^{-1} represents $k_{app(D\rightarrow I)}$. Resemblance of the values of $k_{app(D\rightarrow I)}$ and $k_{app(D\rightarrow E)}$ of DMMBP(A52C)$_{Cy3}$ indicates that SR398-assisted DMMBP(A52C)$_{Cy3}$ folding obeys the tethering scheme. The lower value of k_{GroEL} (0.23 min^{-1}) than k_{in} (0.32 min^{-1}) estimated from $k_{app(D\rightarrow I)}$ may imply that the released intermediate **I** was denatured upon recaptured by chaperonin in iterative GroEL-assisted folding.

To probe the conformational state during folding, a cysteine pair of DMMBP(D184C/K362C), which are located closely (*8*), was labelled with donor and acceptor fluorescent dyes and single-pair FRET was monitored (Fig. 5D, Supplementary Fig. S4B and C). In this experiment, we used SR1, a single ring version of GroEL, which has the same kinetic behaviours as SR398 (*14*). The FRET efficiency of GroEL-assisted

folding of labelled DMMBP increased at a rate (0.23 min^{-1}) that is identical to k_{GroEL} obtained from tryptophan fluorescence (0.23 min^{-1}). In contrast to a previous report (*8*), and consistent with the tethering scheme, DMMBP in the cage started its folding from a more extended conformation than in the case of spontaneous folding, as indicated by a smaller value of FRET efficiency (0.56 ± 0.01) than the value of the spontaneous one (0.61 ± 0.01) (Fig. 5D). The curves of FRET efficiency change in two different concentrations of DMMBP were the same (Supplementary Fig. S4C, cyan and blue), indicating that high initial E_{FRET} is not caused by aggregation.

Folding of DapA also obeys the tethering mechanism

DapA is a typical obligate substrate protein in *Escherichia coli* that requires GroEL and GroES for its folding (*17*, *31*, *32*). DapA mutant containing C20A and a cysteine pair of T3C and E223C, which are located close in the native structure (Fig. 6A), were labelled with the donor (Alexa350) and acceptor fluorescence dyes (Atto488) for single-pair FRET. To measure the folding and escape of monomer DapA and to restrict FRET between monomers in the assembled native tetramer, labelled DapA was mixed with non-labelled DapA at the ratio of 1:4 in following experiments. Escape kinetics observed by the increase of FRET of labelled Atto488 dye on DapA(C20A/T3C/E223C) induced by its binding to trap$(D87K)_{Tx}$ show that 13% of DapA escape out of the cage at an apparent rate $k_{app(D\rightarrow E)}$ of 5.1 min^{-1} (Fig. 6B). Under the condition of spontaneous folding, dilution of urea-denatured DapA immediately produced a rather compact conformational state with single-pair FRET efficiency of 0.66 ± 0.01 and further change did not occur (Fig. 6C and Supplementary Fig. S4D). In chaperonin-assisted DapA folding, folding of labelled DapA started from a state with FRET efficiency of 0.56 ± 0.01, indicating more extended state than spontaneous condition. As folding proceeds, the increasing FRET efficiency approached a value of native DapA (0.82 ± 0.01) (Supplementary Fig. S4D). Because labelled DapA is unable to fold spontaneously (*17*), the FRET increase mostly reflects in-cage folding and its apparent rate, 7.3 min^{-1}, corresponds to $k_{app(D\rightarrow I)}$. As the case of BFP and DMMBP, FRET efficiency change corresponding to $k_{I\rightarrow F}$ was not observed, suggesting that **I** has a near-native conformation. Therefore, the values of $k_{app(D\rightarrow I)}$ and $k_{app(D\rightarrow E)}$ are close enough, though not the same, to justify the tethering scheme. The state formed under spontaneous folding condition is competent as a substrate protein for chaperonin-assisted folding; by addition of GroEL, FRET efficiency shifted down and subsequent addition of ATP induced an increase of FRET efficiency obeying almost identical kinetics observed for the control GroEL-assisted folding (Supplementary Fig. S4D). The curves of FRET efficiency change in two different concentration of DapA were the same (Supplementary Fig. S4D, cyan and blue), indicating that high initial E_{FRET} is not caused by aggregation formation.

Discussion

The common tethered intermediate in chaperonin-assisted folding

We have proposed that denatured protein in the chaperonin cage is tethered to the cage wall, partly protruding out of the cage, and some fraction of denatured protein spontaneously escapes out of the cage (*10*, *14*). This tethering scheme assumes that the in-cage folding and the escape of denatured polypeptide occur from the common tethered intermediate (Fig. 1) (*10*, *15*). However, an alternative scheme is possible that the escape is a result of abortive encapsulation, that is, two types of the tethered intermediates, productive one and abortive one, are formed upon encapsulation of the substrate protein, each leading independently to the in-cage folding and the escape (Supplementary Fig. S1). The difference of these reaction scheme appears in the reaction kinetics, *i.e.* two apparent rate constants of the in-cage release and the escape should be always identical in the tethering scheme, but not in the alternative scheme. Kinetic analysis showed that

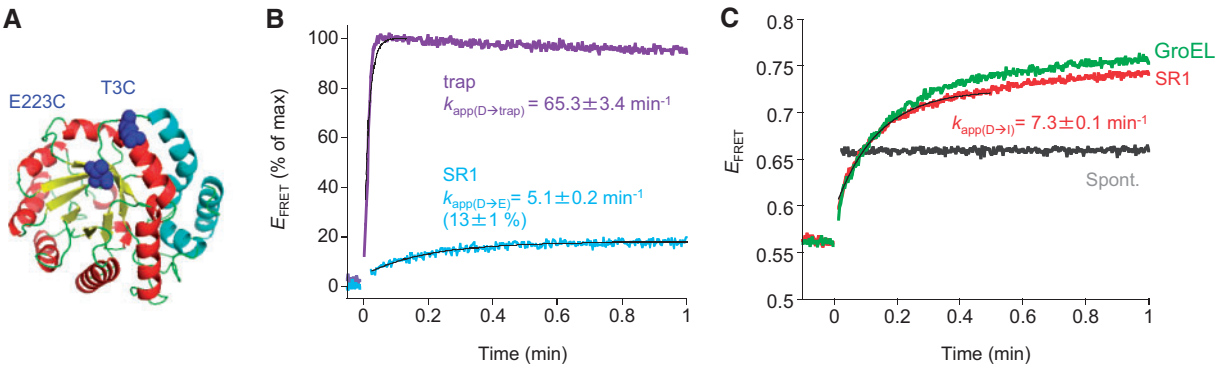

Fig. 6 Chaperonin-assisted folding of DapA. **(A)** Mutated residues of DapA used for single-pair FRET. The monomer structure of DapA is shown in cartoon model (PDBID: 1DHP). T3 and E223 mutated to cysteine are shown in blue CPK model. **(B)** Time course of the escape of DapA. FRET between donor-acceptor labelled DapA(C20A/T3C/E223C) and trap$(D87K)_{Tx}$ are shown as percent of maximum FRET efficiency obtained when denatured DapA was added to trap$(D87K)_{Tx}$/GroES/ATP (purple). The fitting curves giving the indicated rate constants are coloured in black. **(C)** DapA folding monitored by change of single-pair FRET efficiency (E_{FRET}) between fluorescent dyes labelled at T3C/E223C. Spontaneous folding, SR1-assited folding, GroEL-assisted folding are shown in grey, red and green, respectively. The fitting curve to SR1-assisted folding is coloured in black.

the two apparent rate constants are always sufficiently close each other in the folding of BFP, DMMBP and DapA. Previous analysis of chaperonin-assisted folding of rhodanese also indicates similar relationships between the two apparent rate constants (k_{app} = 0.11 min^{-1}, $k_{app(D\rightarrow E)}$ = 0.10 min^{-1}) (*10*). The kinetic analysis, therefore, provides the evidence for the tethering scheme shown in Fig. 1.

The effect of conformational change of polypeptide upon encapsulation

The tethered intermediate is also generated when native Rubisco monomer within the cage is denatured by heat (Fig. 3). Thus, the polypeptide tethering is an intrinsic nature of the chaperonin cage and occurs by itself whenever a denatured protein exists in the cage. When compared with usual in-cage folding reaction starting from encapsulation, the rate of folding starting from Rubisco denatured within the cage and the folding yield are quite similar. Therefore, encapsulation process, *i.e.* binding of ATP and GroES to GroEL loaded with denatured protein and release of denatured protein into the cage, has no or little effect on the folding reaction of Rubisco. It has been reported that, upon binding of GroES, the denatured protein undergoes transiently compaction or extension (*5*, *13*, *19*, *33–35*) and the conformation of the apical domain of GroEL changes (*36*). Our results indicate that the conformational change of denatured protein upon GroES binding does not largely affect the conformation of tethered intermediate and subsequent folding reaction. For the proteins analysed in this study, the iterative reaction by wild-type GroEL did not accelerate protein folding more than that of SR variants. The proposed iterative annealing scheme including forced unfolding of substrate protein by GroEL at each reaction cycle, if any, would be less effective than constant extension by tethering in the closed cage.

The extension of polypeptide by tethering in the cage

As suggested from the results supporting the tethering model, the conformational state of denatured proteins in the tethered intermediate is more extended than that of spontaneous folding. Actually, within the time resolution limit of the single-pair FRET experiment, BFP, DMMBP and DapA started their folding from extended conformations in the chaperonin cage, whereas their spontaneous folding started from compact conformations (Fig. 7). The extended conformation of Rubisco and DMMBP in chaperonin-assisted folding was previously reported but it was thought to be lasted only for a short period (*5*, *33–35*). In contrast, this study indicates that the extended conformation is kept in the chaperonin cage. The extended conformation is consistent with the tethering model, but not with previous assumption that the encapsulated protein is free or repulsive to the cage (*7*, *8*, *29*, *37*). The compact conformation observed in the spontaneous folding reflects the collapsed state which is usually formed at the beginning of spontaneous folding in <20 ms (*25–28*). It is thought that the collapsed state often falls into kinetically-trapped state containing non-native interactions at local energy minimum (*26*, *27*). Therefore, it is considered that chaperonin facilitates protein folding by avoiding initial polypeptide collapse at the expense of possible escape of polypeptide out of the chaperonin cage. However, it should be noticed that the tethering is not always beneficial for acceleration of protein folding. When tethering manner is not suitable (too strong, too many tethered positions, or unfavourable for productive partial folding etc.), productive folding would be delayed and in-cage folding could be slower than spontaneous folding as observed for rhodanese and mouse dihydrofolate reductase (*10*, *38*). Similarly, labelling of the cage wall by hydrophobic fluorescence dyes, which favours interaction with unfolded polypeptide, results in retardation of folding of rhodanese while a risk of the escape decreases (*10*, *39*). When native interactions in polypeptide are more stable than the tethering, the rate of chaperonin-assisted folding is similar to that of spontaneous folding as observed for wild-type MBP (*29*). This folding manner is recognized as passive Anfinsen cage model.

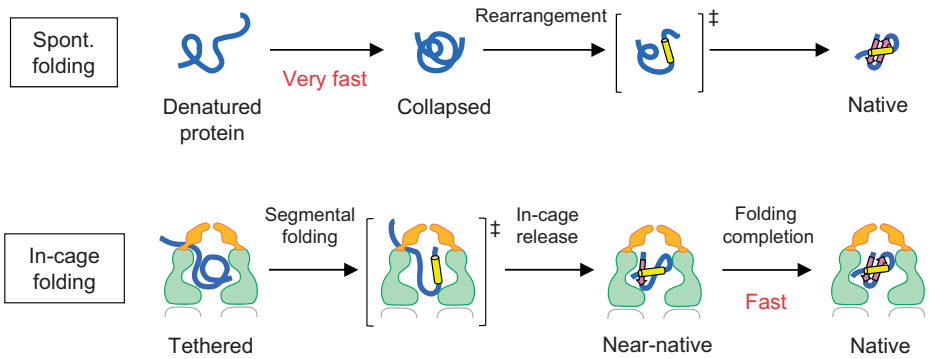

Fig. 7 Difference between spontaneous and in-cage folding. In spontaneous folding, denatured protein collapses rapidly to a compact form (<20 ms) and rearrangement of intramolecular native interactions to form the rate-limiting transition state ensemble (‡) follows (upper scheme). In-cage folding, on the contrary, denatured protein is dynamically tethered to the chaperonin cage wall with more or less extended form and thus avoids the initial collapse (lower scheme). Segmental folding of free portions of polypeptide away from the tethered position follows to form the rate-limiting transition state ensemble (‡). The released near-native intermediate rapidly folds into native state. The rate-limiting transition state ensembles (‡) of spontaneous folding and in-cage folding could be different if the strength of tethering is larger than that of native interactions spontaneously formed in denatured protein.

Previous our study showed that polypeptide was tethered on the hydrophobic residues located at the GroEL–GroES interfaces and GroEL subunit interfaces (*10*). Y203 located at the interface of GroEL subunit is indeed an important residue for protein folding acceleration and the inhibition of polypeptide escape (*10*). It has been reported that the hydrophobic C-terminal tail of GroEL interacts with denatured protein and facilitates protein folding (*12*, *13*, *40*). The simulation study suggested that hydrophobic interaction between denatured protein and the cage is strong enough to unfold rhodanese and removes nonnative interactions within rhodanese (*41*).

The facilitation of segmental folding by tethering

By virtue of real-time monitoring of BFP folding, we clarify that the spontaneous folding proceeds through single step from compact conformation and in contrast, the in-cage folding proceeds through two steps; in-cage release of the tethered protein and folding completion of the released protein to native structure. The second step is rapid and it appears that the tethered polypeptide gains a near-native structure by the time it is untethered, leaving only the final step of folding (Fig. 7). The tethered position is shifting quickly and there may be a moment when polypeptide is tethered to a position suitable for the freely mobile portion of polypeptide to generate native-like partial structure. The partial structures thus formed may have some stability and tend to accumulate. Then, free polypeptide region available for tethering becomes narrowed and finally whole protein becomes free to finish folding. In support of this, we observed previously the burst of folding completion in the cage upon untethering by reduction of disulphide bond which covalently tethered rhodanese to the cage wall (*42*). Because a burst size increases as the incubation time before untethering increases, it is clear that partial, productive folding proceeds even in the tethered polypeptide. A recent extensive study reveals efficient, sequential progress of segmental folding of DapA in the chaperonin cage, not in the spontaneous folding (*17*). In addition, Ye *et al*. (*30*) recently reported that chaperonin facilitated the formation of hydrophobic core but slowed the conformational search at the slowest folding region in MBP(V8G) mutant. The residues (D184C and K362C) used for FRET measurement of DMMBP are located in the slowest folding region. Their result could be explained by above reaction scheme, that is, the tethering of unstable region reduces the nonnative interaction to the core structure and facilitates its formation. Certainly, these observations reflect the segmental folding of the tethered polypeptide in the cage.

Supplementary Data

Supplementary Data are available at *JB* Online.

Acknowledgements

We are grateful to Y. Ishizaki and Y. Motojima-Miyazaki for protein preparation.

Funding

This work was supported by MEXT-supported Programme for the Strategic Research Foundation at Private Universities (2011-2016), and Grant-in-Aid for Scientific Research (C) (No. JP15K06983 to F. M.).

Conflict of Interest

None declared.

References

1. Hartl, F.U., and Hayer-Hartl, M. (2002) Molecular chaperones in the cytosol: from nascent chain to folded protein. *Science* **295**, 1852–1858
2. Fenton, W.A., and Horwich, A.L. (2003) Chaperonin-mediated protein folding: fate of substrate polypeptide. *Q. Rev. Biophys.* **36**, 229–256
3. Ellis, R.J. (1994) Molecular chaperones. Opening and closing the Anfinsen cage. *Curr. Biol.* **4**, 633–635
4. Horwich, A.L., Apetri, A.C., and Fenton, W. a. (2009) The GroEL/GroES cis cavity as a passive anti-aggregation device. *FEBS Lett.* **583**, 2654–2662
5. Shtilerman, M., Lorimer, G.H., and Englander, S.W. (1999) Chaperonin function: folding by forced unfolding. *Science* **284**, 822–825
6. Stan, G., Thirumalai, D., Lorimer, G.H., and Brooks, B.R. (2003) Annealing function of GroEL: structural and bioinformatic analysis. *Biophys. Chem.* **100**, 453–467
7. Tang, Y.C., Chang, H.C., Chakraborty, K., Hartl, F.U., and Hayer-Hartl, M. (2008) Essential role of the chaperonin folding compartment in vivo. *Embo J.* **27**, 1458–1468
8. Chakraborty, K., Chatila, M., Sinha, J., Shi, Q., Poschner, B.C., Sikor, M., Jiang, G., Lamb, D.C., Hartl, F.U., and Hayer-Hartl, M. (2010) Chaperonin-catalyzed rescue of kinetically trapped states in protein folding. *Cell* **142**, 112–122
9. Motojima, F., Makio, T., Aoki, K., Makino, Y., Kuwajima, K., and Yoshida, M. (2000) Hydrophilic residues at the apical domain of GroEL contribute to GroES binding but attenuate polypeptide binding. *Biochem. Biophys. Res. Commun.* **267**, 842–849
10. Motojima, F., and Yoshida, M. (2010) Polypeptide in the chaperonin cage partly protrudes out and then folds inside or escapes outside. *Embo J.* **29**, 4008–4019
11. Xu, Z., Horwich, A.L., and Sigler, P.B. (1997) The crystal structure of the asymmetric GroEL-GroES-(ADP)7 chaperonin complex. *Nature* **388**, 741–750
12. Chen, D.-H., Madan, D., Weaver, J., Lin, Z., Schröder, G.F., Chiu, W., and Rye, H.S. (2013) Visualizing GroEL/ES in the act of encapsulating a folding protein. *Cell* **153**, 1354–1365
13. Weaver, J., and Rye, H.S. (2014) The C-terminal tails of the bacterial chaperonin GroEL stimulate protein folding by directly altering the conformation of a substrate protein. *J. Biol. Chem.* **289**, 23219–23232
14. Motojima, F., Motojima-Miyazaki, Y., and Yoshida, M. (2012) Revisiting the contribution of negative charges on the chaperonin cage wall to the acceleration of protein folding. *Proc. Natl. Acad. Sci. U. S. A.* **109**, 15740–15745
15. Motojima, F. (2015) How do chaperonins fold protein? *Biophysics (Oxford)* **11**, 61–70
16. Motojima, F., and Yoshida, M. (2003) Discrimination of ATP, ADP, and AMPPNP by chaperonin GroEL: hexokinase treatment revealed the exclusive role of ATP. *J. Biol. Chem.* **278**, 26648–26654

17. Georgescauld, F., Popova, K., Gupta, A.J., Bracher, A., Engen, J.R., Hayer-Hartl, M., and Hartl, F.U. (2014) GroEL/ES chaperonin modulates the mechanism and accelerates the rate of TIM-barrel domain folding. *Cell* **157**, 922–934
18. Makino, Y., Amada, K., Taguchi, H., and Yoshida, M. (1997) Chaperonin-mediated folding of green fluorescent protein. *J. Biol. Chem.* **272**, 12468–12474
19. Rye, H.S., Burston, S.G., Fenton, W.A., Beechem, J.M., Xu, Z., Sigler, P.B., and Horwich, A.L. (1997) Distinct actions of cis and trans ATP within the double ring of the chaperonin GroEL. *Nature* **388**, 792–798
20. Weissman, J.S., Rye, H.S., Fenton, W.A., Beechem, J.M., and Horwich, A.L. (1996) Characterization of the active intermediate of a GroEL-GroES-mediated protein folding reaction. *Cell* **84**, 481–490
21. Rye, H.S., Roseman, A.M., Chen, S., Furtak, K., Fenton, W.A., Saibil, H.R., and Horwich, A.L. (1999) GroEL-GroES cycling: aTP and nonnative polypeptide direct alternation of folding-active rings. *Cell* **97**, 325–338
22. Ueno, T., Taguchi, H., Tadakuma, H., Yoshida, M., and Funatsu, T. (2004) GroEL mediates protein folding with a two successive timer mechanism. *Mol. Cell* **14**, 423–434
23. Suzuki, M., Ueno, T., Iizuka, R., Miura, T., Zako, T., Akahori, R., Miyake, T., Shimamoto, N., Aoki, M., Tanii, T., Ohdomari, I., and Funatsu, T. (2008) Effect of the C-terminal truncation on the functional cycle of chaperonin GroEL: implication that the C-terminal region facilitates the transition from the folding-arrested to the folding-competent state. *J. Biol. Chem.* **283**, 23931–23939
24. Apetri, A.C., and Horwich, A.L. (2008) Chaperonin chamber accelerates protein folding through passive action of preventing aggregation. *Proc. Natl. Acad. Sci. U. S. A.* **105**, 17351–17355
25. Agashe, V.R., Shastry, M.C., and Udgaonkar, J.B. (1995) Initial hydrophobic collapse in the folding of barstar. *Nature* **377**, 754–757
26. Dobson, C.M., and Karplus, M. (1999) The fundamentals of protein folding: bringing together theory and experiment. *Curr. Opin. Struct. Biol.* **9**, 92–101
27. Daggett, V., and Fersht, A.R. (2003) Is there a unifying mechanism for protein folding? *Trends Biochem. Sci.* **28**, 18–25
28. Walters, B.T., Mayne, L., Hinshaw, J.R., Sosnick, T.R., and Englander, S.W. (2013) Folding of a large protein at high structural resolution. *Proc. Natl. Acad. Sci. U. S. A.* **110**, 18898–18903
29. Tang, Y.-C.C., Chang, H.-C.C., Roeben, A., Wischnewski, D., Wischnewski, N., Kerner, M.J., Hartl, F.U., and Hayer-Hartl, M. (2006) Structural features of the GroEL-GroES nano-cage required for rapid folding of encapsulated protein. *Cell* **125**, 903–914
30. Ye, X., Mayne, L., Kan, Z., and Englander, S.W. (2018) Folding of maltose binding protein outside of and in GroEL. *Proc. Natl. Acad. Sci. U. S. A.* **115**, 519–524
31. Kerner, M.J., Naylor, D.J., Ishihama, Y., Maier, T., Chang, H.-C., Stines, A.P., Georgopoulos, C., Frishman, D., Hayer-Hartl, M., Mann, M., and Hartl, F.U. (2005) Proteome-wide analysis of chaperonin-dependent protein folding in Escherichia coli. *Cell* **122**, 209–220
32. Fujiwara, K., Ishihama, Y., Nakahigashi, K., Soga, T., and Taguchi, H. (2010) A systematic survey of in vivo obligate chaperonin-dependent substrates. *Embo J.* **29**, 1552–1564
33. Lin, Z., Madan, D., and Rye, H.S. (2008) GroEL stimulates protein folding through forced unfolding. *Nat. Struct. Mol. Biol.* **15**, 303–311
34. Sharma, S., Chakraborty, K., Muller, B.K., Astola, N., Tang, Y.C., Lamb, D.C., Hayer-Hartl, M., and Hartl, F.U. (2008) Monitoring protein conformation along the pathway of chaperonin-assisted folding. *Cell* **133**, 142–153
35. Lin, Z., and Rye, H.S. (2004) Expansion and compression of a protein folding intermediate by GroEL. *Mol. Cell.* **16**, 23–34
36. Motojima, F., Chaudhry, C., Fenton, W.A., Farr, G.W., and Horwich, A.L. (2004) Substrate polypeptide presents a load on the apical domains of the chaperonin GroEL. *Proc. Natl. Acad. Sci. U. S. A.* **101**, 15005–15012
37. Takagi, F., Koga, N., and Takada, S. (2003) How protein thermodynamics and folding mechanisms are altered by the chaperonin cage: molecular simulations. *Proc. Natl. Acad. Sci. U. S. A.* **100**, 11367–11372
38. Hofmann, H., Hillger, F., Pfeil, S.H., Hoffmann, A., Streich, D., Haenni, D., Nettels, D., Lipman, E.A., and Schuler, B. (2010) Single-molecule spectroscopy of protein folding in a chaperonin cage. *Proc. Natl. Acad. Sci. U. S. A.* **107**, 11793–11798
39. Madan, D., Lin, Z., and Rye, H.S. (2008) Triggering protein folding within the GroEL-GroES complex. *J. Biol. Chem.* **283**, 32003–32013
40. Weaver, J., Jiang, M., Roth, A., Puchalla, J., Zhang, J., and Rye, H.S. (2017) GroEL actively stimulates folding of the endogenous substrate protein PepQ. *Nat. Commun.* **8**, 1–15
41. Sirur, A., and Best, R.B. (2013) Effects of interactions with the GroEL cavity on protein folding rates. *Biophys. J.* **104**, 1098–1106
42. Motojima, F., and Yoshida, M. (2015) Productive folding of a tethered protein in the chaperonin GroEL-GroES cage. *Biochem. Biophys. Res. Commun.* **466**, 72–75